Web-based Supplementary Materials for Improved Dynamic Predictions from Joint Models of Longitudinal and Survival Data with Time-Varying Effects using P-splines by Eleni-Rosalina Andrinopoulou, Paul H.C. Eilers, Johanna J.M. Takkenberg and Dimitris Rizopoulos

Web Appendix A

The following sections represent figures, tables and discussion regarding the analysis of the data and the simulations. More specifically,

- Web Figure 1 presents the profile of the square root of aortic gradient (SAG) for 12 randomly selected patients.
- Web Table 1 and 2 present the results of the varying-coefficient joint model (VCJM) and the constant-coefficient joint model (CCJM), respectively.
- Web Figure 2 and 3 present the trace plots of the association parameters of the VCJM.
- Web Appendix B consist of a discussion of the results of the models.
- Web Appendix C consist of the likelihood of the survival submodel.
- Web Figure 4 presents the dynamic survival/intervention-free predictions for patient 10.
- Web Figure 5 presents the SAG evolution for patient 10.
- Web Table 3 presents the simulation scenarios.
- Web Figure 6 presents the results of the simulation from Scenario I when fitting the VCJM with 8 internal knots.
- Web Figure 7 presents the results of the simulation from Scenario I when fitting the VCJM with 20 internal knots.
- Web Figure 8 presents the results of the simulation from Scenario II when fitting the VCJM with 8 internal knots.

- Web Figure 9 and 10 present the results of the simulation from Scenario IIIa and Sceniario IIIb when fitting the VCJM with 8 internal knots.

Web Figure 1

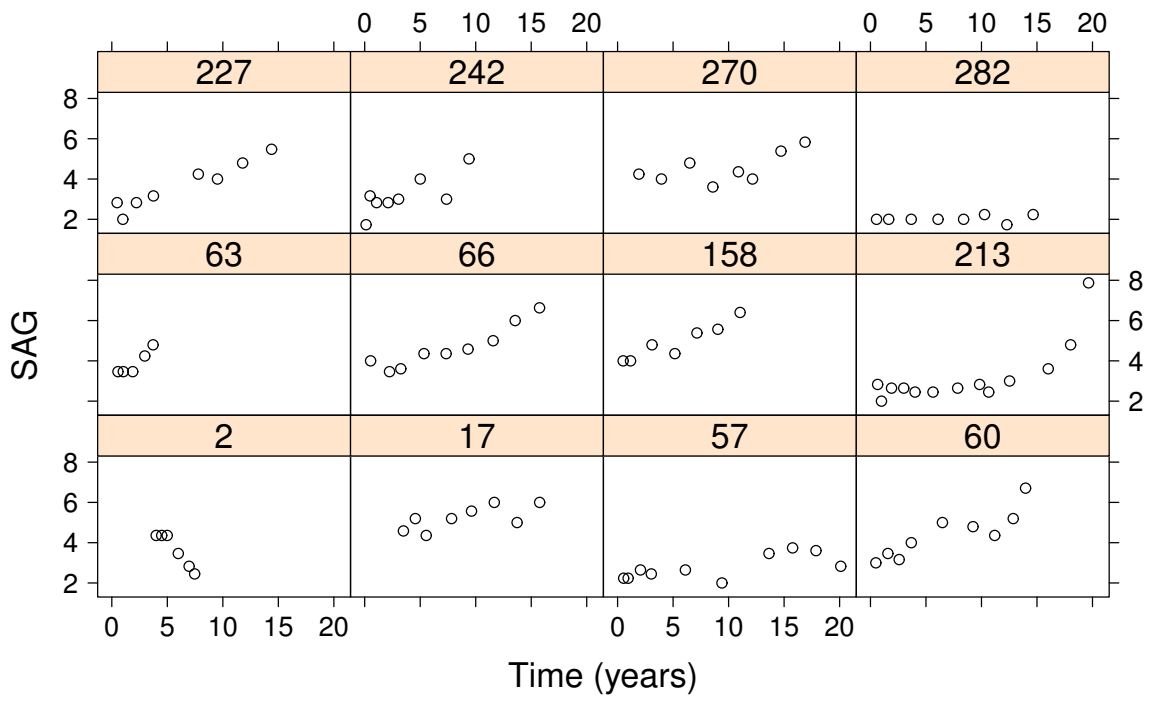

Figure 1: Profile of the SAG for 12 randomly selected patients.

Web Table 1

Table 1: VCJM results: posterior means, standard errors and 95% credible intervals

	Mean	SE	2.5%	97.5%
Serum bilirubin				
SexMale	3.02	0.08	2.86	3.17
SexFemale	3.19	0.11	2.97	3.41
ns(echotime, 2)1	3.81	0.29	3.27	4.37
ns(echotime, 2)2	3.38	0.36	2.73	4.14
Survival				
Sex	0.003	0.19	-0.38	0.37
alpha value[1]	0.01	0.27	-0.54	0.52
alpha value[2]	0.04	0.20	-0.34	0.43
alpha alue[3]	0.07	0.14	-0.21	0.36
alpha value[4]	0.09	0.11	-0.12	0.30
alpha value[5]	0.11	0.10	-0.09	0.29
alpha value[6]	0.13	0.10	-0.08	0.31
alpha value[7]	0.13	0.12	-0.10	0.35
alpha value[8]	0.13	0.14	-0.14	0.41
alpha value[9]	0.18	0.18	-0.18	0.55
alpha value[10]	0.23	0.25	-0.24	0.75
alpha slope[1]	0.86	1.72	-2.76	4.03
alpha slope[2]	1.94	1.31	-0.68	4.41
alpha slope[3]	3.02	1.10	0.88	5.23
alpha slope[4]	4.10	1.20	1.99	6.71
alpha slope[5]	5.18	1.55	2.63	8.71
alpha slope[6]	6.25	2.03	3.00	11.04
alpha slope[7]	7.32	2.56	3.30	13.44
alpha slope[8]	8.39	3.11	3.51	15.87
alpha slope[9]	9.46	3.69	3.67	18.29
alpha slope[10]	10.53	4.27	3.79	20.78
DIC				8818.89

Web Table 2

Table 2: CCJM results: posterior means, standard errors and 95% credible intervals

	Mean	SE	2.5%	97.5%
Serum bilirubin				
SexMale	3.01	0.08	2.87	3.16
SexFemale	3.20	0.11	2.98	3.42
ns(echotime, 2)1	3.83	0.26	3.32	4.35
ns(echotime, 2)2	3.35	0.31	2.75	4.00
Survival				
Sex	-0.01	0.18	-0.37	0.34
alpha value	0.11	0.06	-0.004	0.24
alpha slope	3.14	0.83	1.62	4.86
DIC				8909.496

Web Figure 2

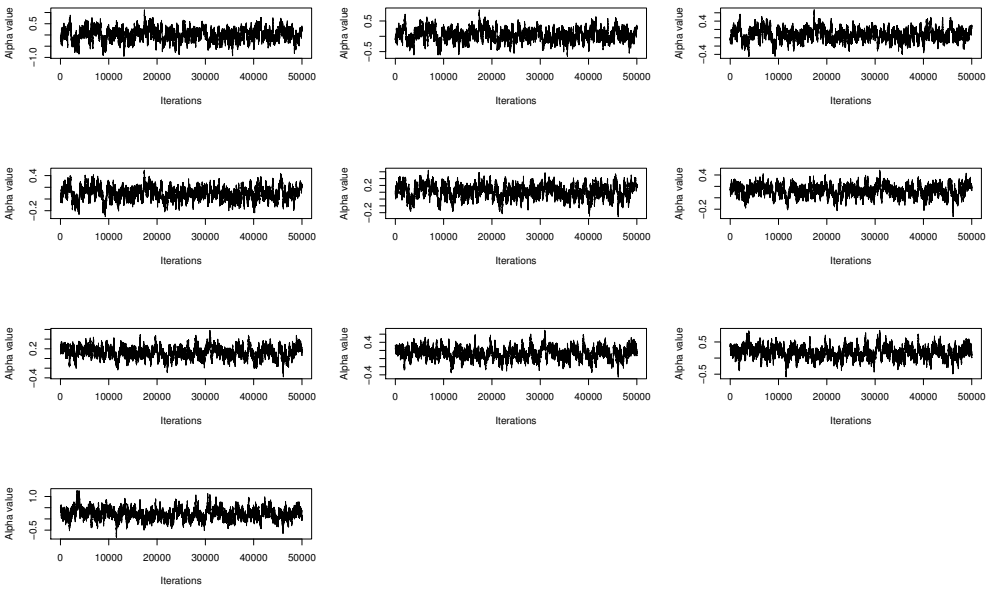

Figure 2: Trace plots for the underlying value parameters of the SAG from the VCJM.

Web Figure 3

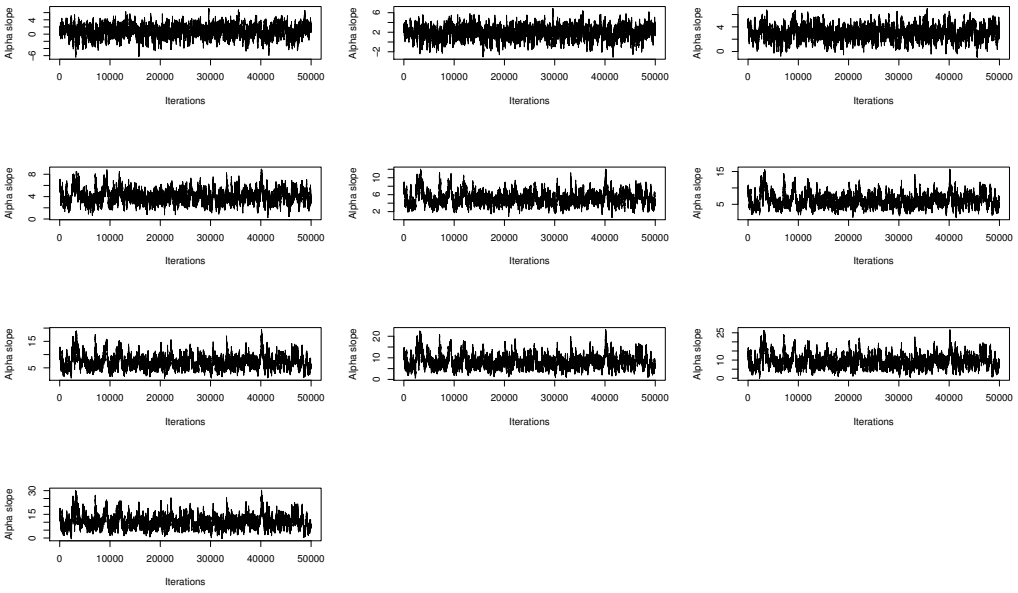

Figure 3: Trace plots for the slope parameters of the SAG from the VCJM.

1 Web Appendix B

In Web Table 1 and 2 we present posterior means, standard errors and 95% credible intervals of the VCJM and CCJM respectively. With regards to the VCJM, it can be seen that gender seems to be a strong factor for the SAG. Specifically, females are associated with a higher SAG. A nonlinear effect of time seems to capture the evolution of SAG. Furthermore, gender does not seem to have an influence on the survival outcome. The results of the association parameters are difficult to interpret therefore plots were created in the manuscript (Figure 2 in the main paper) where it can be seen that the slope of the SAG on survival appears to increase linearly with time. With regards to the CCJM, we found the same results for the longitudinal submodel as in the VCJM. Moreover, gender and the underlying value of the SAG do not seem to have an influence on the survival outcome. The underlying slope of the SAG seems to have an effect on the survival outcome. In particular, the log hazard is increased by 3.14, with 95% credible interval [1.62, 4.86], for each unit increase in the current slope of the SAG. The DIC values indicate that the VCJM provides a better fit of the data compared to the CCJM. Finally, Web Figure 2 and 3 suggest that the association parameters

of the VCJM converged.

2 Web Appendix C

The likelihood contribution of the survival model is given by

$$
\begin{aligned}
&p\{T_i, \delta_i \mid \eta_i(T_i), \boldsymbol{\theta}_s\} = \\
&\quad \exp\Bigg[\sum_{q=1}^{Q} \gamma_{h_0,q} B_q(T_i, \boldsymbol{\nu}) + \gamma^\top \boldsymbol{w}_i + f\{\sum_{l=1}^{L} \alpha_l B_l(T_i), \eta_i(T_i)\}\Bigg]^{I(\delta_i=1)} \times \\
&\quad \exp\Bigg\{-\exp\left(\boldsymbol{\gamma}^\top \boldsymbol{w}_i\right) \int_0^{T_i} \exp\Bigg[\sum_{q=1}^{Q} \gamma_{h_{0k},q} B_q(s, \boldsymbol{\nu}) + f\{\sum_{l=1}^{L} \alpha_l B_l(s), \eta_i(s)\}\Bigg] ds\Bigg\}.
\end{aligned}
$$

The integral of the survival function does not have a closed-form solution, and thus a numerical method must be employed for this evaluation. To approximate this integral we used the Gaussian quadrature rule and we assume a 15-point Gauss-Kronrod rule.

Web Figure 4

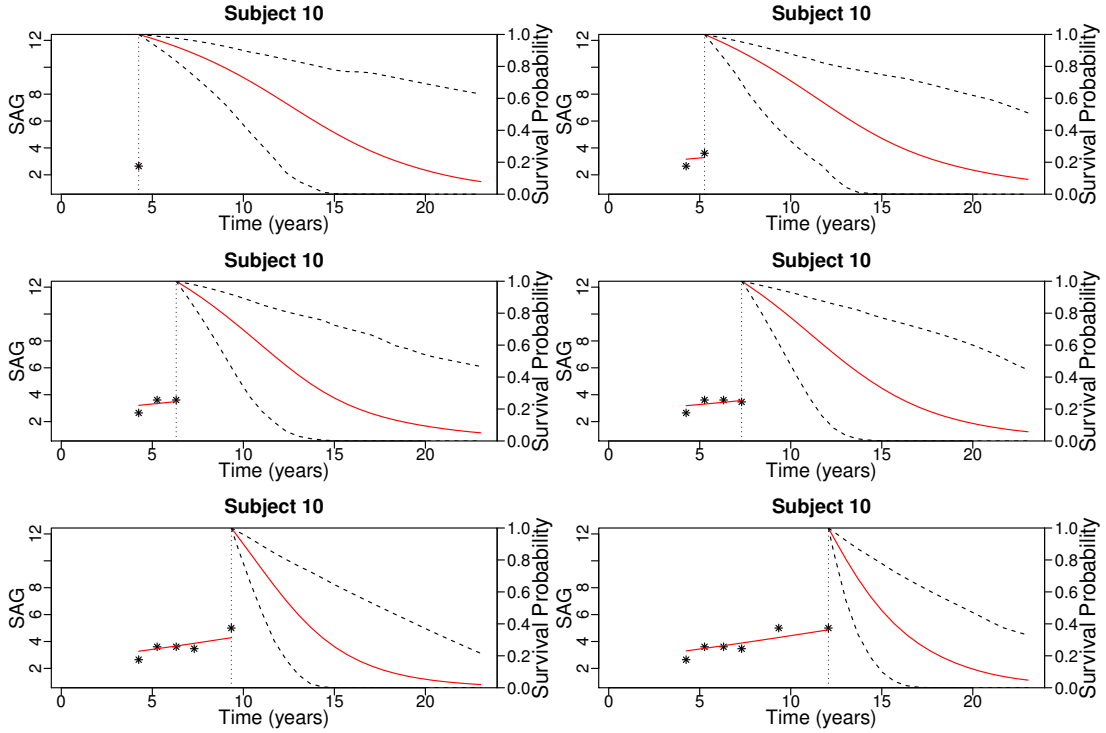

Figure 4: Dynamic survival/intervention-free predictions for patient 10. The vertical dotted lines represent the time point of the last SAG measurement. On the left side, the fitted longitudinal trajectory is presented. On the right side, the solid line represents the mean estimator of the predictions while the dashed lines the corresponding 95% confidence interval.

Web Figure 5

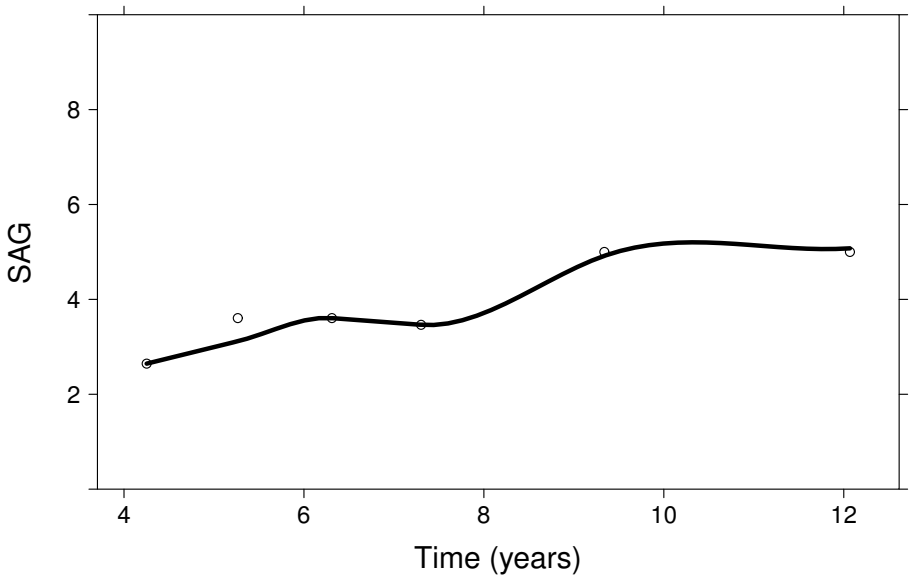

Figure 5: The SAG evolution for patient 10.

Web Table 3

Table 3: Simulation scenarios.

Scenario	$\boldsymbol{\beta}$	$\boldsymbol{\sigma}_y$	$diag\{\boldsymbol{\Sigma}_b\}$	ξ	μ_c	$\boldsymbol{\gamma}$	$\boldsymbol{\alpha}$
Ia							
	(Intercept) = 3.03	0.69	0.93	1.2	30	(Intercept) = -7.85	0.19
	Females = 0.14		0.16			Females =-0.02	0.35
	Time = 0.16						0.5
							0.9
							1.3
							1.9
							2.2
							2.59
							2.9
							3.19
Ib							
	(Intercept) = 3.03	0.69	0.93	1.2	30	(Intercept) = -7.75	0.19
	Females = 0.14		0.16			Females =-0.02	0.35
	Time = 0.16						0.4
							0.6
							0.9
							1
							2.2
							2.59
							2.9
							3.19
II							
	(Intercept) = 3.03	0.69	0.93	1.9	24	(Intercept) = -7.85	0.38
	Females = 0.14		0.16			Females =-0.02	
	Time = 0.16						
IIIa							
	(Intercept) = 3.02	0.69	0.93	1.7	12	(Intercept) = -5.75	-0.89
	Females = 0.16		0.16			Females = 0.01	0.26
	Time = 0.16						-0.01
IIIb							
	(Intercept) = 3.02	0.69	0.93	1.7	12	(Intercept) = -5.75	-1.33
	Females = 0.16		0.16			Females = 0.01	0.75
	Time = 0.16						-0.15
							0.01
							-0.0002

Web Figure 6

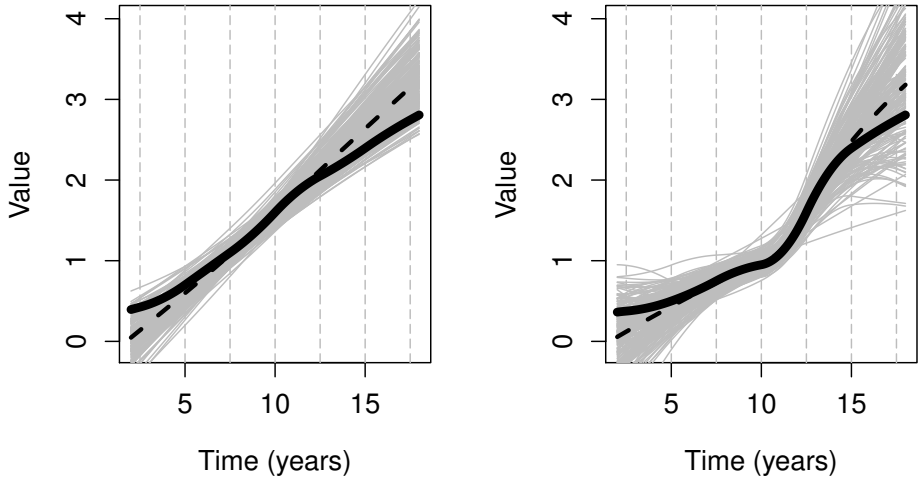

Figure 6: Simulation results assuming a time-varying effect (Scenario I) and 8 internal knots when simulating and assuming the VCJM with the same knots when fitting the data: the left panel corresponds to Scenario Ia (linear $\lambda(t)$) and the right panel to Scenario Ib (non-linear $\lambda(t)$). The solid black lines denote the true $\lambda(t)$ function, the dashed black lines the average estimates of this function from the 200 data sets and the grey lines the estimates from each of the 200 data sets.

Web Figure 7

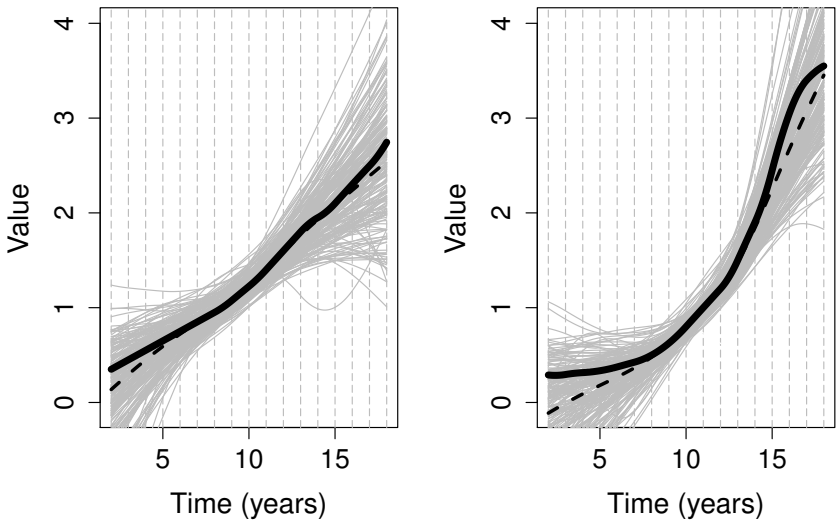

Figure 7: Simulation results assuming a time-varying effect (Scenario I) and 20 internal knots when simulating and assuming the VCJM with the same knots when fitting the data: the left panel corresponds to Scenario Ia (linear $\lambda(t)$) and the right panel to Scenario Ib (non-linear $\lambda(t)$). The solid black lines denote the true $\lambda(t)$ function, the dashed black lines the average estimates of this function from the 200 data sets and the grey lines the estimates from each of the 200 data sets.

Web Figure 8

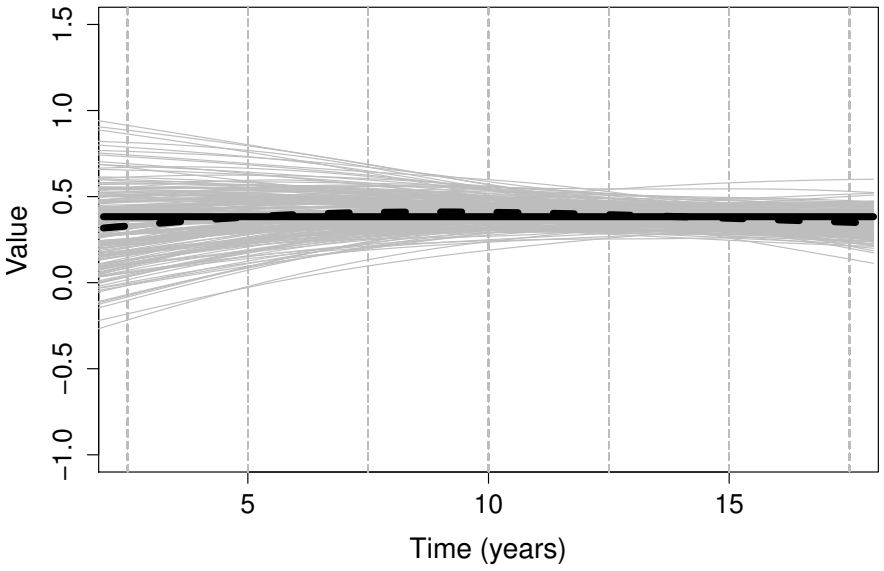

Figure 8: Simulation results assuming a constant effect (Scenario II) when simulating and assuming the VCJM with 8 internal knots when fitting the data: The solid black lines denote the true association parameter, the dashed black lines the average estimates of this function from the 200 data sets and the grey lines the estimates from each of the 200 data sets.

Web Figure 9

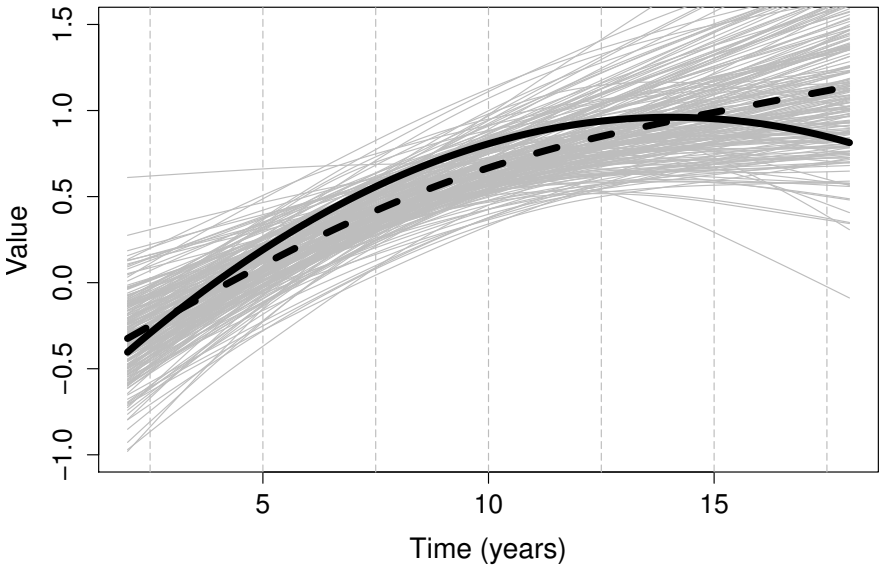

Figure 9: Simulation results assuming a second degree polynomial for the time function of the time-varying coefficient (Scenario IIIa) when simulating and assuming the VCJM with 8 internal knots when fitting the data: The solid black lines denote the true association parameter, the dashed black lines the average estimates of this function from the 200 data sets and the grey lines the estimates from each of the 200 data sets.

Web Figure 10

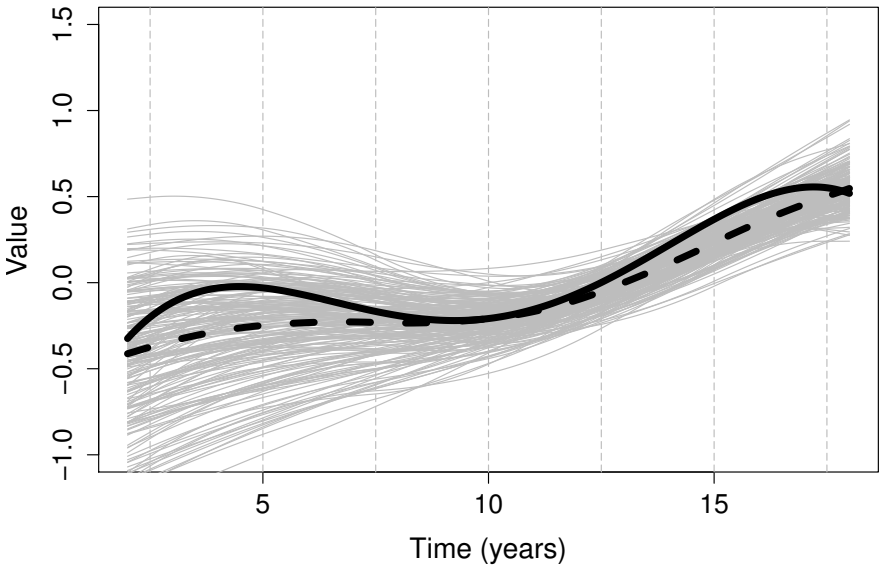

Figure 10: Simulation results assuming a fourth degree polynomial for the time function of the time-varying coefficient (Scenario IIIb) when simulating and assuming the VCJM with 8 internal knots when fitting the data: The solid black lines denote the true association parameter, the dashed black lines the average estimates of this function from the 200 data sets and the grey lines the estimates from each of the 200 data sets.